

Unsupervised Feature Learning for Environmental Sound Classification Using Cycle Consistent Generative Adversarial Network

Mohammad Esmaeilpour, Patrick Cardinal, Alessandro L. Koerich

*École de Technologie Supérieure, Université du Québec
1100 Notre-Dame West, Montréal, QC, H3C 1K3, Canada.*

Abstract

In this paper we propose a novel environmental sound classification approach incorporating unsupervised feature learning from codebook via spherical K -Means++ algorithm and a new architecture for high-level data augmentation. The audio signal is transformed into a 2D representation using a discrete wavelet transform (DWT). The DWT spectrograms are then augmented by a novel architecture for cycle-consistent generative adversarial network. This high-level augmentation bootstraps generated spectrograms in both intra and inter class manners by translating structural features from sample to sample. A codebook is built by coding the DWT spectrograms with the speeded-up robust feature detector (SURF) and the K -Means++ algorithm. The Random Forest is our final learning algorithm which learns the environmental sound classification task from the clustered codewords in the codebook. Experimental results in four benchmarking environmental sound datasets (ESC-10, ESC-50, UrbanSound8k, and DCASE-2017) have shown that the proposed classification approach outperforms the state-of-the-art classifiers in the scope, including advanced and dense convolutional neural networks such as AlexNet and GoogLeNet, improving the classification rate between 3.51% and 14.34%, depending on the dataset.

Email addresses: mohammad.esmaeilpour.1@ens.etsmtl.ca (Mohammad Esmaeilpour), patrick.cardinal@etsmtl.ca (Patrick Cardinal), alessandro.koerich@etsmtl.ca (Alessandro L. Koerich)

Keywords: Environmental sound classification, generative adversarial network (GAN), Cycle-Consistent GAN, K-means++, and Random Forest.

1. Introduction

Environmental sound classification has been attracted the interest of several researchers in machine learning because of its vast applications [1, 2, 3]. However, this is a challenging problem due to the complex nature of environmental recordings in terms of dimensionality, different mechanism of sound production, overlapping of different sources, and lack of high-level structures usually observed in speech and in many types of musical sounds [4]. This complex nature masked by natural acoustic noises [5] can make the classification of specific sounds very challenging. This challenge becomes more sensible when audio classes do not have similar sound production mechanisms such as "car horn" and "car engine idling" in open scenes like streets or parks [6, 1, 7].

In the literature, the classification of environmental sounds has been addressed using both standalone and ensemble classification setups incorporating conventional classifiers and deep neural networks where the input signal can be represented by a waveform (1D) or converted to a mid-level representation (2D) such as a spectrogram [8, 9, 10, 11, 4, 12, 13]. The audio signal may also be represented by hand-crafted features using the spectral or the cepstral domain mainly via frequency transformations which are lossy in terms operation. Zero-crossing rate [14], spectral flux and centroid [15], chroma vector [16], Mel frequency cepstral coefficients (MFCCs) [17], short-time Fourier transform (STFT) [18], cross recurrent plot (CRP) [19], and DWT [20] are among the most well-known hand-crafted features for audio classification [21]. These hand-crafted features not only reduce the dimensionality of the audio signal but may also reduce some types of noise and help to extract time-varying descriptors towards finer discrimination. Performance-wise, the approaches that use these features have shown relatively better performance compared to approaches that use directly 1D signals in both classification and clustering tasks, mainly when employing conventional classifiers such as support vector machines (SVMs) [22].

MFCC is a common and reliable informative representation format for analyzing audio and for this reason, most of the proposed classification approaches in this domain rely on it [23, 24, 25, 2]. MFCCs, which are based on the human auditory system, are hand-crafted features which can make a reasonable balance between handling the complex nature of real-life sounds and providing informative feature vectors for classification/clustering purposes. In addition to traditional classifiers such as Gaussian mixture models [26], hidden Markov models [27] and K -nearest neighbor [28], convolutional neural networks (ConvNets) [29] have been evaluated on MFCC feature vectors and achieved better results than the 1D audio signal format. However, MFCCs have shown to be very sensitive to background noise and this might affect the performance of classifiers for noisy environmental sounds [30].

With the recent advances in deep learning, many strong classifiers such as ConvNets have been introduced, which are designed to learn directly both from 1D and 2D data. ConvNets are quite similar to dense deep neural network (DNN) with the main difference of including convolution layer(s) to deal with raw data. These layers act as a feature detector and can help regular DNNs to achieve better discrimination boundaries. The main advantage of these networks is their ability to learn directly from raw data rather than hand-crafted features. ConvNets have been used with audio waveforms with several convolution layers incorporating different 1D signal augmentation methods [12]. Experimental results have shown competitive accuracy compared to unsupervised sound classifiers [4], ConvNets on MFCCs [31], and sometimes better performance [32] depending on the the dataset. ConvNets has also been experimented with a combination of 1D and MFCC feature vectors which resulted in low classification error [13]. This shows the importance of the representation space in extracting discriminating features.

Due to the high dimensionality of sounds, training classifiers on 2D representation(s) of real-life sounds is preferred over raw waveforms. Although, ConvNets have shown great classification performances in 1D signal format (in an end-to-end setup) [12], so far, they could not outperform AlexNet and GoogLeNet on spectrograms generated

by STFT, DWT, and CRP transformations [33]. The majority of published papers in audio classification especially environmental sounds are on 2D representations mainly for DNNs such as the networks introduced in [29]. STFT, DWT, and CRP are the main approaches for producing 2D representations (known as spectrograms) for a given audio recording. There are also some algorithms which combine these three representations such as [34]. They show the importance of having more spectrograms so as to extract more informative 2D representations for training dense ConvNets by augmenting sounds. It has been shown that STFT and DWT have more competence for extracting temporal and structural content for ConvNets [35]. For some common environmental datasets, two dense ConvNets as GoogLeNet and AlexNet have achieved the highest recognition accuracy with quite high confidence.

However, one of the main bottlenecks for using ConvNets in environmental sound classification is the amount of data required to train such networks properly due to the high number of parameters to adjust. The two main approaches that have been used to circumvent this problem is fine-tuning ConvNets pretrained on other domains/datasets and generating artificial samples by data augmentation. Both 1D and 2D data augmentation [36, 33] have been proposed for improving classification performance which proves the importance of providing better input rather than implementing high complex and costly networks such as [10]. There are several algorithms for augmenting a dataset both in terms of enhancing samples' visual quality and quantity. Augmentation in 2D representations like spectrograms is mostly being implemented with low-level transformations [37] including translation, shearing, rotation, scaling, aspect ratio, flipping, etc., which in general may not improve the performance of conventional or advanced deep learning classifiers. The linear nature of these affine transformations may not cause a high impact on the classifier decision boundaries [38]. It is worth mentioning that, even those low-level data augmentations have been sometimes contributed significantly in training ConvNets and reducing overfitting.

Elastic deformation [39] is another low-level augmentation which has been shown

promising results in optical character recognition using supervised classifiers. The elastic distortion implements a similarity transformation which interpolates between highly correlated spectrogram submanifolds. When the dimensions of the spectrogram samples are small, and they do not have much active areas (super uniform areas in pixel-wise level), this augmentation may not work well especially for deep learning models. Extracting covariant patches and color space channel intensity alteration [40] as well as other types of pixel-level augmentation scheme has been utilized in many spectrogram classification tasks and they have proven their potential in finely bootstrapping spectrograms.

In addition to the linear nature of low-level augmentation, they cannot enhance data distribution which is usually determined by high-level features. Some methodologies have been proposed for rectifying this problem such as learning multivariate normal distribution for each class with respect to their mean manifolds [41]. Implementation of this augmentation in the real world, especially for long audio representations with high dimensions is not optimal. One potential solution could be multivariate distribution learning in representation space [42] with respect to the structural components [43] of a spectrogram.

In this paper, we propose a novel approach for environmental sound classification which has four main steps: (i) sound dimension conversion and preprocessing (from 1D to 2D); (ii) data augmentation using a novel architecture for the cycle-consistent generative adversarial network; (iii) extracting feature vectors from the augmented dataset via SURF algorithm and organizing them into a codebook; and (iv) training a random forest algorithm on the resulting codebook. The experimental results have shown that our approach outperforms cutting-edge dense classifiers such as AlexNet and GoogLeNet in four benchmarking environmental sound datasets: ESC-10, ESC-50, UrbanSound8K and DCASE-2017. The main contribution of this paper is a proposed architecture for data augmentation which translates a spectrogram to another using a generative model, namely cycle-consistent generative adversarial network. Experimental results show the remarkable performance of this data augmentation method for the unsupervised feature

learning.

The organization of this paper is as follows. In Section 2 we firstly discuss about the transformation of audio waveforms (1D) into spectrograms (2D), as well as the preprocessing steps preceding and succeeding such a transformation for augmentation purposes. Section 3 presents the Cycle-Consistent Generative Adversarial Network (GAN) for high-level spectrogram augmentation so as to bootstrapping structural components. In Section 4 we explain our feature learning methodology using SURF descriptors and the spherical K -means++ algorithm, and also the classification approach based on random forests that learns from codebooks. Section 5 provides details about the architecture of the proposed cycle-consistent GAN and experiments carried out in four datasets. The conclusions and future work are presented in the last section.

2. Preprocessing and Spectrogram Generation

In this section we present the preprocessing steps for augmenting the given input audio data before converting them to spectrograms, as well as the strategy used to generate the spectrograms.

2.1. 1D Data Augmentation

Given the relatively small size of the environmental sound datasets, one of the recommended steps before transforming an audio waveform to a 2D representation is data augmentation to boost the amount, distribution, and cardinality of the samples of each class in the datasets. Data augmentation can be carried out by applying some filters on the audio signal such as pitch shifting, time stretching, compressing dynamic range, and eliminating background noise (noise removal filters) [12]. Since these augmentation filters increase the number of samples of the dataset, they may have potential to affect the performance of data-driven classifiers. Obviously, this effect is quite relevant to the characteristics of the sound dataset.

It has been shown [34] that the pitch-shifting filter alone can highly boost the quality of audio recordings compared to applying all the above-mentioned augmentation filters

as proposed in [12]. After conducting several exploratory experiments, we have found out that, for most of the environmental sound datasets applying all 1D data augmentation filters do not necessarily produce good audio samples (in terms of producing samples with less similarity inter classes and high in inter.) Therefore, we only use the pitch-shifting augmentation as its constructive effects have been shown in [12] for both supervised and unsupervised feature learning. For such an aim, we use static pitch shifting scales [44]. This boosts the number of samples in the dataset with respect to the number of applied scales.

2.2. Spectrogram Generation

As stated before, STFT, DWT, and CRP are the main approaches for producing spectrograms for a given audio recording. ConvNets have shown strong capability in learning from these spectrograms either standalone [33] or pooled together [34]. However, based on some exploratory experiments with environmental sound datasets we may say that the DWT representation is more stable to time warping deformations and it can better characterize time varying structures compared to other representations such as STFT and CRP or even their combinations. The STFT transformation is somewhat similar to DWT in terms of producing low and high frequency components encoded as spectrograms. Considering a discretized sound signal $x[t]$ distributed over time t , then its DWT transformation is:

$$\text{DWT}(x[n]) = (x \otimes g)[n] = \sum_{k=-\infty}^{\infty} x[k]g[n-k] \quad (1)$$

where the convolution of $x[t]$ and $g[.]$, denoted as \otimes , which is known as the mother function, produces other signals which can be either low or high pass filter sets. This operation can be applied to at most the minimum length of $x[t]$. The 2D representation of this signal can be achieved via Eq. 2.

$$S_{\text{DWT}}\{x[t]\} \equiv |\text{DWT}(x[n])|^2 \quad (2)$$

where S_{DWT} denotes the spectrogram of the signal $x[t]$.

We generate DWT spectrograms using our modified version of the sound explorer C++ script [45] for the original audio signals as well as the pitch-shifted audio samples, so as to handle audio clips with any length (time duration).

2.3. Spectrogram Enhancement

Each generated spectrogram is a 2D array of intensity values which can be noisy when its associated audio signal is affected by environmental noise(s). In this case, adjusting the distribution of the intensity values can help to extract/learn more informative features [46].

For improving the color space and the dynamic color contrast of the intensity values, we apply a histogram equalization filter [47]. Considering each pixel intensity of the generated spectrogram S as $S(i, j)$, then the enhanced spectrogram (S_{heq}) will be defined in Eq. 3.

$$S_{heq}(i, j) = \left[(s - 1) \sum_{i=0}^{S(i,j)} p_i \right] \quad (3)$$

where s is the supremum of 8-bit precision and p_i denotes to the ratio of pixels with intensity i over the total number of pixels. This filter expands the intensity range of a given spectrogram in a balanced distribution. In the following subsection we explain how to structurally augment the generated spectrograms towards more informative samples.

3. Cycle-Consistent Generative Adversarial Network

The methodology proposed for augmenting generated spectrograms in the current study is based on cycle-GAN which maps one spectrogram to another spectrogram as the efficiency of this 2D-to-2D translation has been proven in the literature [48, 49]. Our augmentation pipeline will be implemented only in 2D space since mapping 1D-to-1D audio signal for augmentation purposes is very challenging due to the high dimensionality of audio recordings.

Our perspective in data augmentation is directed towards increasing inter and intra class structural contents over low-level pixel augmentations. This can help classifiers to reach a finer decision boundary among data submanifolds with minimum overlap. This type of augmentation is known as image-to-image translation. A more accurate way to impose structural contents on data augmentation is by using GAN since we can consistently control the mapping process from one image to another by adding an extra constraint to its loss function(s).

The importance of the high-level augmentation is more tangible for spectrograms because compared to regular computer vision datasets (e.g. ImageNet [50]), spectrograms do not have solid object(s) sensitive to low-level transformations. Moreover, the total number of samples in environmental sound dataset are limited and image-to-image translation using Cycle-Consistent GAN can effectively boost the size and the quality of the dataset.

All GAN architectures consist of two networks of generator (G) and discriminator (D) where they capture data distribution and estimate the probability that a sample comes from the training data rather than G , respectively. The G in a standard GAN generates fake data from latent variables with respect to the distribution of real training data, whereas in Cycle-Consistent GAN [49] it bijectively translates an input sample from a source S to a target T . In other words, this type of GAN has two generators and two discriminators which are trained independently. The original architecture of Cycle-Consistent GAN is shown in Fig. 1a.

In this paper we focus on both paired (when S is similar to T ; or equivalently intra-class translation) and unpaired (when S and T are somewhat similar to each other or; equivalently inter-class translation) Cycle-Consistent GAN. For the latter, we propose a pipeline for properly selecting source and target spectrograms with respect to the confusion matrix of the classifier. This high-level augmentation transfers structural components from the source spectrogram S to the target spectrogram T . If the Cycle-Consistent GAN is trained carefully, it can produce spectrogram samples that may help

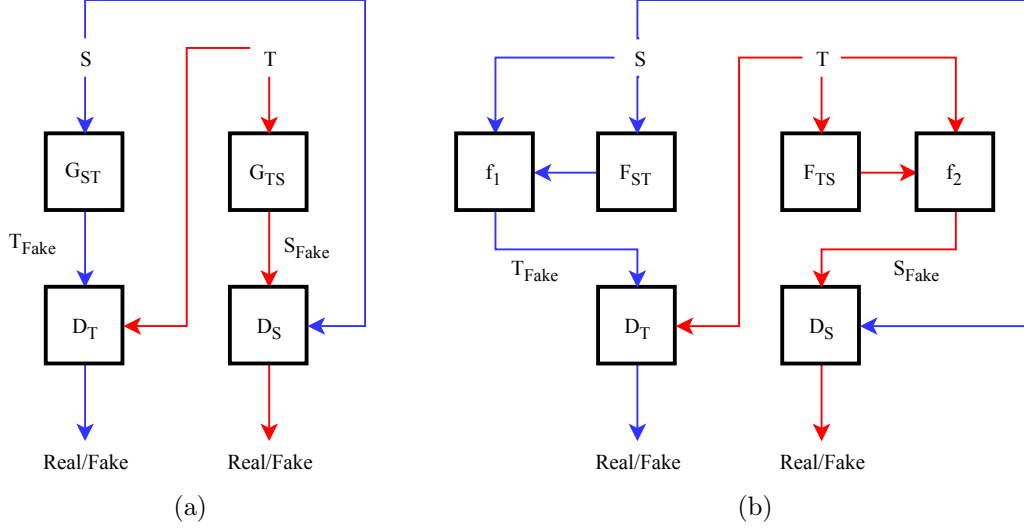


Figure 1: (a): Illustration of the original Cycle-Consistent GAN for image-to-image translation where the cycle consistency imposes $G_{ST}(S_{Fake}) \approx T$ and $G_{TS}(T_{Fake}) \approx S$. (b): Our proposed Cycle-Consistent GAN inspired from [51]. Generators in our framework are F_{ST} and F_{TS} equivalent to G_{ST} and G_{TS} , respectively.

improve the performance of a classifier trained with such samples.

Producing realistic (natural-looking) spectrograms by the Cycle-Consistent GAN is not one of our priorities since any sort of spectrogram do not have much meaning for human-eye. Interestingly, generated spectrogram using our generator network may not produce samples similar to the given sources, but discriminator shows reasonable sensitivity to it (matches the target label). Some examples of generated samples are depicted in Fig. 4. Forcing generators to produce very similar samples will result in divergences in the cycle consistency optimization. This condition for cycle-consistent GANs mostly apply for augmenting datasets to which the human-eye perceives some structure like MNIST and ImageNet.

In Figure 1-a, G_{ST} and G_{TS} stand for generators translating samples from $S \rightarrow T$ and $T \rightarrow S$, respectively. D_T and D_S denote the modules for discriminating real samples from generated fake samples from G_{ST} and G_{TS} . This can be achieved by optimizing

the following criterion:

$$G_{S \rightarrow T} = \arg \min_{G_{S \rightarrow T}} \max_{D_T} \mathcal{L}_{GAN}(G_{S \rightarrow T}, D_T) \quad (4)$$

where the loss function \mathcal{L}_{GAN} is defined in Equation 5.

$$\begin{aligned} \mathcal{L}_{GAN}(G_{S \rightarrow T}, D_T) = & \mathbb{E}_{t \sim p_{target(t)}} [\log D_{T(t)}] + \\ & \mathbb{E}_{s \sim p_{source(s)}} [\log(1 - D_{T(t)}(G_{S \rightarrow T}(s)))] \end{aligned} \quad (5)$$

where $p_{target(t)}$ and $p_{source(s)}$ denote the sample distributions in the target T and in the source S , respectively. The common problem with this definition of loss function is gradient vanishing as explained in [52] which makes training and convergence almost impossible. To circumvent this problem, in our proposed Cycle-Consistent GAN architecture depicted in Figure 1-b, we use a least-square loss function for GAN (LSGAN) as proposed in [53] for different domains S and T as given in Equations 6 and 7:

$$\begin{aligned} \mathcal{L}_{LSGAN}(F_{S \rightarrow T}, D_T) = & \mathbb{E}_{t \sim p_{target(t)}} [(D_{T(t)} - 1)^2] + \\ & \mathbb{E}_{s \sim p_{source(s)}} [D_{T(t)}(F_{S \rightarrow T}(s))^2] \end{aligned} \quad (6)$$

$$\begin{aligned} \mathcal{L}_{LSGAN}(F_{T \rightarrow S}, D_S) = & \mathbb{E}_{s \sim p_{target(s)}} [(D_{S(s)} - 1)^2] + \\ & \mathbb{E}_{t \sim p_{source(t)}} [D_{S(s)}(F_{T \rightarrow S}(t))^2] \end{aligned} \quad (7)$$

Though these loss functions minimize the approximated Jensen-Shannon divergence between two distributions of legitimate and generated data [54], they oversmooth the spectrograms. Oversmoothing affects the performance of the discriminator towards a wrong label other than the predefined target label. For rectifying this problem, we bypass the inputs to the discriminator. Hence, we propose to add two modules depicted in Figure 1-b as f_1 and f_2 , which act as weighted bypasses (identity mapping) to the

discriminators. The definitions of these two modules are provided in Equations 8 and 9.

$$f_1 = c_1 \odot S + \mu \odot F_{ST} \quad (8)$$

$$f_2 = c_2 \odot T + \sigma \odot F_{TS} \quad (9)$$

where dimensions of the generators and the input/target are bilinearly interpolated to match each other. The \odot denotes the element-wise multiplication. The values of the constants c_1 and c_2 , and the variables μ and σ are obtained empirically upon several experiments. Basically, f_1 and f_2 bypass connections have two main advantages in our proposed high-level augmentation setup. Firstly, the low-to-high compensations because regular Cycle-Consistent GAN (Fig. 1a) translates a randomly picked distribution from a low-dimension (e.g. pixel-level noisy sample) to a higher dimension which is a realistic image. Assuming that the dimension of the random drawn distribution is not very large, and no optimization overhead is involved (in the case of an optimal generator [55]), then potentially the following cycle-consistency criterion can yield to a realistic fake sample:

$$\begin{aligned} \mathcal{L}_{cycle}(G_{S \rightarrow T}, G_{T \rightarrow S}) = & \mathbb{E}_{s \sim p_{source(s)}} [\|G_{T \rightarrow S}(G_{S \rightarrow T}(s) - s)\|_1] \\ & + \mathbb{E}_{t \sim p_{target(t)}} [\|G_{S \rightarrow T}(G_{T \rightarrow S}(t) - t)\|_1] \end{aligned} \quad (10)$$

where $\|\cdot\|_1$ is the L_1 norm. This might converge to a saddle point (where the minimax game in GAN is over) when the Kullback-Leibler divergence $\mathbb{KL}(p_{source(s)}, p_{target(t)}) \approx \mathbb{KL}(p_{target}, p_{source})$. In other words, the similarity between the source and the target distribution should be high. When the similarity between samples is not high enough especially when they have been drawn from different classes, Equation 10 can no longer result in realistic fake images. The f_i bypasses can overcome this problem by providing more information from the given legitimate input.

The second advantage of embedding f_1 and f_2 into our proposed Cycle-Consistent GAN is the ability of sharpening features that may have been oversmoothed during translation (especially in the discriminator domain). Finally, the total loss criterion

which will be optimized in our augmentation scenario is given in Eq. 11:

$$\mathcal{L}_{total}(F_{S \rightarrow T}, F_{T \rightarrow S}, D_S, D_T) = \mathcal{L}_{LSGAN}(F_{S \rightarrow T}, D_T) + \mathcal{L}_{LSGAN}(F_{T \rightarrow S}, D_S) + \alpha \mathcal{L}_{cycle}(F_{S \rightarrow T}, F_{T \rightarrow S}) \quad (11)$$

where α is a scaling parameter for balancing the cycle whose value is also set manually upon experiments. The architectures of our proposed $F_{S \rightarrow T}$ and $F_{T \rightarrow S}$ are depicted in Fig. 2 where they both are multi-layered ConvNets. These architectures are not general but totally dependent on the type of problem and dataset.

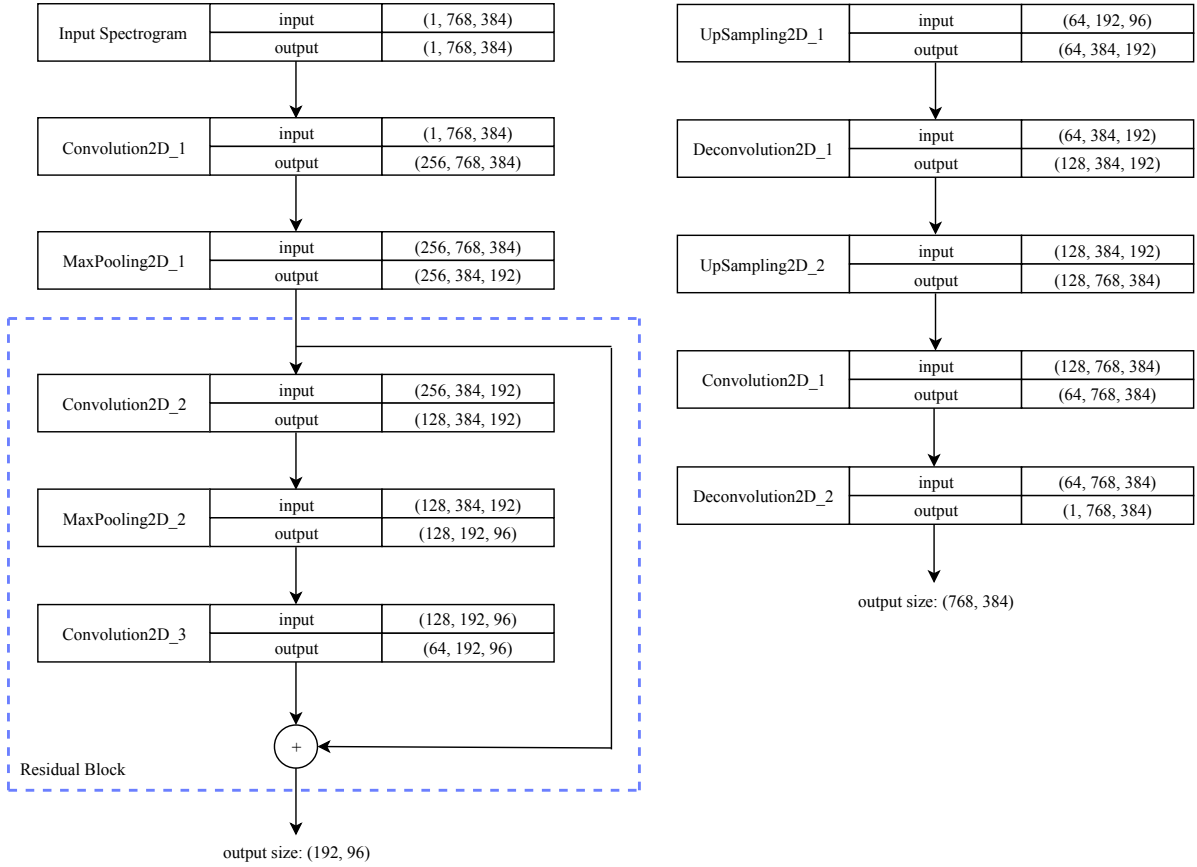


Figure 2: Generator architectures for DWT spectrograms: **left:** $F_{S \rightarrow T}$, and **right:** $F_{T \rightarrow S}$. Values inside of parentheses indicate the number of filters, height, and width of the spectrogram, respectively.

3.1. ConvNets Architecture for Cycle-Consistent GAN

Assuming that we generate DWT spectrograms with the fixed dimension of 768×384 , for high-level augmentation using a Cycle-Consistent GAN, we propose the architectures

illustrated in Figure 2 for the generators ($F_{S \rightarrow T}$, $F_{T \rightarrow S}$). The residual network shown in Figure 2 may have from three to seven residual blocks [56], depending on the dataset. Each residual block contains two convolution layers and one bypassing residual connection. In all the layers depicted in Fig. 2 the convolutions come with receptive field of 3×3 and stride 1×1 . Also, the sizes of the generated outputs in the residual blocks are bilinearly interpolated to match each other.

For discriminator functions D_T and D_S we use one single architecture as depicted in Figure 3. In this proposed architecture we again set the receptive field to 3×3 and strides are set to 1×1 and 2×2 for the first and second convolution layers, respectively.

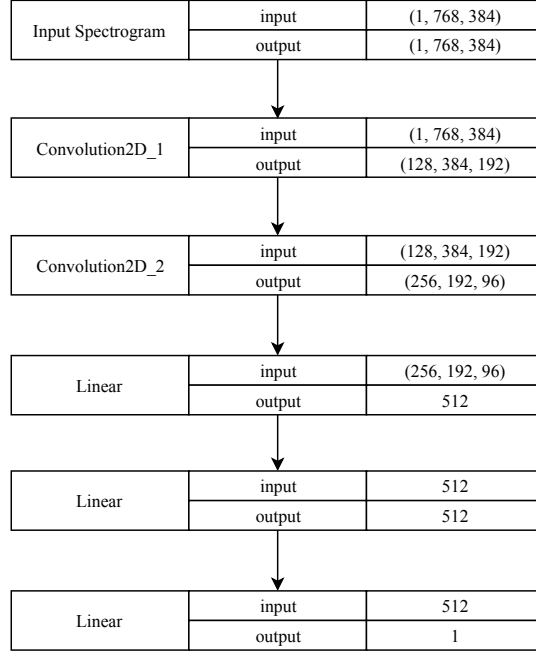


Figure 3: Network architecture for D_T and D_S .

4. Unsupervised Feature Learning and Classification

The proposed approach for classifying DWT spectrograms is based on an unsupervised feature learning from a codebook. In this section, we introduce how to extract and encode features from spectrograms into a codebook and explain how to organize them into several clusters. Finally, we train a classifier on top of the clusters.

4.1. Feature Encoding

For extracting feature vectors, the speeded up robust feature (SURF) [57] is implemented which is the modified version of the scale invariant feature transform (SIFT) [58] by fast approximation of Hessian matrix (for encoding principal curvatures at each interest point) and producing integral images from spectrograms. Upon our several experiments (in our classification setup), SURF visual words provide us with better feature vectors compared to MFCC visual words which have been studied for music and environmental sound classifications [4, 59].

Each integral image represents the summation of the given spectrogram pixels of a rectangular region with different sizes so as to produce local features. Using the box filter (for Gaussian approximation) SURF approximates the location and scale of each interest points using the determinant of the weighted Hessian matrix as the following.

$$H(\mathbf{p}, \sigma) \approx \begin{bmatrix} \hat{L}_{xx}(p, \sigma) & \hat{L}_{xy}(p, \sigma) \\ \hat{L}_{xy}(p, \sigma) & \hat{L}_{yy}(p, \sigma) \end{bmatrix} \quad (12)$$

$$\det(H(\mathbf{p}, \sigma)) = \hat{L}_{xx}(p, \sigma)\hat{L}_{yy}(p, \sigma) - [0.9(\hat{L}_{xy}(p, \sigma))]^2 \quad (13)$$

where $\hat{L}_{..x}(p, \sigma)$ is the convolution of the second derivative of Gaussian with the spectrogram $S(x, y)$ at point x , and σ is the Gaussian scale (scale at which the point has been detected). After locating the interest points in space and scale, SURF descriptor can be generated. We divide each region into 16 sub regions (4×4 grids of size 4×4) and compute Haar wavelet responses for obtaining orientation of interest points. In each sub region, we compute differential four-element descriptor vector as Eq. 14.

$$\text{descriptor}_{\text{subregion}} = \left[\sum dx, \sum dy, \sum |dx|, \sum |dy| \right] \quad (14)$$

The length of the regional feature descriptor will be 16×4 which is represented by a 64-dimensional vector. These values are determined empirically and they will not change during the implementation or across datasets. More details are presented in

Section 5. Therefore, each spectrogram is now represented by a 64-dimensional feature vector and in the next step we organize such vectors, also called visual words into a codebook.

4.2. Organizing Visual Words into a Codebook Using Spherical K -Means++

The number of extracted feature vectors over all the given dataset is tremendously high and this negatively affects classifier’s performance. Therefore, representing these vectors with respect to their similarities into centers and organize them into a codebook can considerably improve classification process.

We use the K -Means++ algorithm [60] as an unsupervised feature learning for organizing codewords. This clustering algorithm is adapted from the traditional K -means algorithm where K denotes the number of potential seeds (centroids). This value is usually associated with the number of classes in the audio dataset. The main advantage of the K -Means++ algorithm over the traditional K -means algorithm is that it uses a weighted probability distribution over the data point (feature vector in our case) sub-manifold(s) with probability proportional to its squared distance with its neighbors. This is very useful in our case since the derived feature vectors are not from solid images.

Similar to the traditional K -Means, the K -Means++ algorithm has a super polynomial structure and it might result in null seeds for similar data points [61]. One possible solution provided for K -means is adding an extra optimization constraint to it by binding seeds to have a unit L_2 norm which forces the centroid to roll over a unique sphere. This algorithm is called spherical K -Means [62]. By taking advantage of this extra constraint and embedding it into the K -Means++ clustering algorithm, spherical K -means++ [63] will turn out.

The performance of standard spherical K -Means is studied for specific forms of environmental sound dataset with quite small cardinality [64]. It has been proven that, this clustering algorithm produces competitive results with cutting-edge clustering and other advanced supervised classifiers [65]. Adding a spherical constraint in the distance objective function of K -Means usually results in improving the consistency in producing

centroids.

Considering the feature vectors of an input spectrogram as a $X_{m,n}$ matrix where m and n denote to the number of feature vectors and their dimensionality in form of $1 \times n$, respectively ($i = 1 \cdots m$ and $j = 1 \cdots n$). In Eq. 15 we define z_i for storing the assigned value (mean of centroids) of our K clusters which forms the matrix Z . Finally, our codebook is defined as $V \in \mathbb{R}^{n \times K}$.

$$z_j^i := \begin{cases} V^j x^{i\top} & \text{if } j = \arg \max_l \left| V^l x^{i\top} \right|_{j,i} \text{ and } p(x) \sim cp(d^2(x^i)) \\ 0 & \text{otherwise} \end{cases} \quad (15)$$

where x^i is a row from X and c is a constant value for weighting the square distance of each x^i to its nearest center. Specifically, d and p denote the distance between two feature vectors and their joint probability distribution, respectively, and \top indicates matrix transposition. More details about the basics of spherical K -means algorithm is provided in [62].

$$V := XZ^\top + V, \quad V^j := \frac{V^j}{\|V^j\|_2} \quad \forall j \quad (16)$$

where these two operations in addition to updating centroids, normalize them by L2 norm. We recommend initializing the centroids randomly following the normal distribution. The codebook matrix V contains K organized clusters and in the next subsection we train a classifier on it (codewords of the codebook).

4.3. Classification

For classifying the generated codebook (on its quantized codewords) we use random forest algorithm [66] with a different number of trees. This algorithm is an estimator which fits some decision trees on different subsamples of the given codebook via averaging. We train this algorithm with different sizes of trees (estimators) with respect to the dimensions of the generated codebook. For splitting of a random tree node, the Gini

impurity criterion is used as follows:

$$G = \sum_{i=1}^n p_i(1 - p_i) \quad (17)$$

where n denotes the number of classes in the target variable and p_i is the ratio of each class. The maximum depth of trees varies from 16 to 64 with respect to the type of codebook. Specifically, for codewords associated with long audio recordings, we use deeper trees. The minimum number of samples required to split an internal node is set to $0.02 \times m$ where m stands for the number of samples. The \sqrt{k} with k number of features has been utilized to compute the best ratio for node split.

This classifier has shown great potential for classifying codebooks [67]. Upon our initial experiments, we have noticed that the performance of this classifier is quite lower than codebook without spherical biding of the K -Mean++ algorithm. This indicates the importance of proper codewords organization.

5. Experimental Results

We assess the performance of the proposed classification approach in four environmental sound datasets: UrbanSound8K, ESC-10, ESC-50, and DCASE-2017. The first dataset includes 8,732 audio samples of length up to four seconds, arranged in 10 classes: air conditioner (AI), car horn (CA), children playing (CH), dog bark (DO), drilling (DR), engine idling (EN), gunshot (GU), jackhammer (JA), siren (SI), and street music (SM). The ESC-50 includes 2,000 samples with length of five seconds arranged in 50 classes including major groups of animals, natural sounds capes and water sounds, human non-speech sounds, domestic sounds, and exterior noises. The ESC-10 is a subset of ESC-50 which includes 400 recordings arranged in 10 classes of dog bark, rain, sea waves, baby cry, clock tick, person sneeze, helicopter, chainsaw, rooster, fire crackling. Finally, DCASE-2017 consists of 4,680 10-second audio samples from 15 classes: bus, cafe, car, city center, forest path, grocery store, home, lakeside beach, library, metro station, office (multiple persons), residential area, train, tram, and urban park. Though

the cardinalities of samples per class in UrbanSound8K are not balanced, this dataset contains all the most challenging environmental sounds in real life compared to the other three datasets in terms of including different sound production mechanisms.

After applying low-level augmentations on audio signals using static pitch shifting scales of 0.75, 0.9, 1.15, and 1.5 we produce DWT spectrograms by setting the sampling frequency of the environmental sounds to 8kHz, 16kHz, 8kHz, and 16kHz for ESC-10, ESC-50, UrbanSound8K, and DCASE-2017 datasets respectively. Also, we set the frame length to 50ms for ESC-10 and UrbanSound8K, 30ms for ESC-50, and 40ms for DCASE-2017 with a fixed overlapping size of 50% [34]. For each 1D augmented sample in all datasets, we generate the DWT spectrograms with the fixed dimension of 768×384 . Empirically, this dimension makes a reasonable trade-off between enough information content (in terms of feature vectors) and dimensionality.

Each spectrogram undergoes to the enhancement step, followed by the data augmentation by the proposed cycle-consistent GAN. The ConvNets presented in Fig. 2 have normalized convolution layers by applying instance normalization [68] technique followed by leaky ReLU activation function with slope 0.3. We used Glorot weight normalization algorithm for improving learning. The tentative values for c_1 , c_2 , μ , σ , and α in Eqs. 8, 9, and 11 for different datasets are shown in Table 1.

Table 1: Empirically obtained values for parameters explained in Eqs. 8, 9, and 11.

Dataset	Parameter Values				
	c_1	c_2	μ	σ	α
ESC-10	0.49	0.67	0.02	0.76	0.23
ESC-50	0.39	0.68	0.12	0.58	0.19
UrbanSound8K	0.62	0.36	0.14	0.57	0.03
DCASE-2017	0.03	0.21	0.18	0.43	0.31

For discriminator functions D_T and D_S we use a single architecture as depicted in Fig. 3. In this proposed architecture we set the receptive field to 3×3 and strides are set to 1×1 and 2×2 for the first and second convolution layers, respectively. In this case we used ReLU activation function and batch normalization [69]. These four networks

are trained in four parallel GPUs GTX580 and based on an implementation proposed in [40]. We applied early stopping policy for training these networks and the total number of epochs for training these four networks is shown in Table 2.

Table 2: The total number of training epoch for four networks generators and discriminators.

Dataset	# of Training Epochs			
	$F_{S \rightarrow T}$	$F_{T \rightarrow S}$	D_S	D_T
ESC-10	123	107	104	91
ESC-50	136	118	109	116
UrbanSound8K	112	106	97	45
DCASE-2017	213	143	90	102

In order to produce more structural spectrograms from source S to target T and make the loss functions converge, we first need to have an idea of the relation between samples from inter classes (for intra classes we randomly pick samples because sample similarity in intra classes is naturally high enough). To this aim, we train a random forest algorithm on spectrograms without data augmentation featuring different number of trees from 500 to 3,000 (the best generalization was achieved at 2,000, 1,864, 2,500, 2,496 for ESC-10, ESC-50, UrbanSound8K, and DCASE-2017 respectively). Fig. 5a shows the confusion matrices for the random forest trained with the UrbanSound8K dataset without data augmentation.

The values in Fig. 5a indicate similarities of classes to each other. For instance, class "EN" has the most similarity to the class "AI" because the classifier has been misclassified samples from the class "AI" as class "EN" in 14% of the total cases. Therefore, we set the source and target classes in Fig. 1 to $S = "AI"$ and $T = "EN"$, respectively. We continue this procedure for all the classes. In addition to intra class image-to-image translation, we augment the generated DWT spectrograms in inter-class manner as well. We select randomly 50% of samples within a class as the source and the remaining 50% as the target classes. Overall, we boost the size of the dataset to extra 1,500, 2,000, 5,000 and 4,500 for ESC-10, ESC-50, UrbanSound8K and DCASE-2017 respectively.

In Fig. 5a the highest confusions are between classes "SM" and "CH" (20% + 6%)

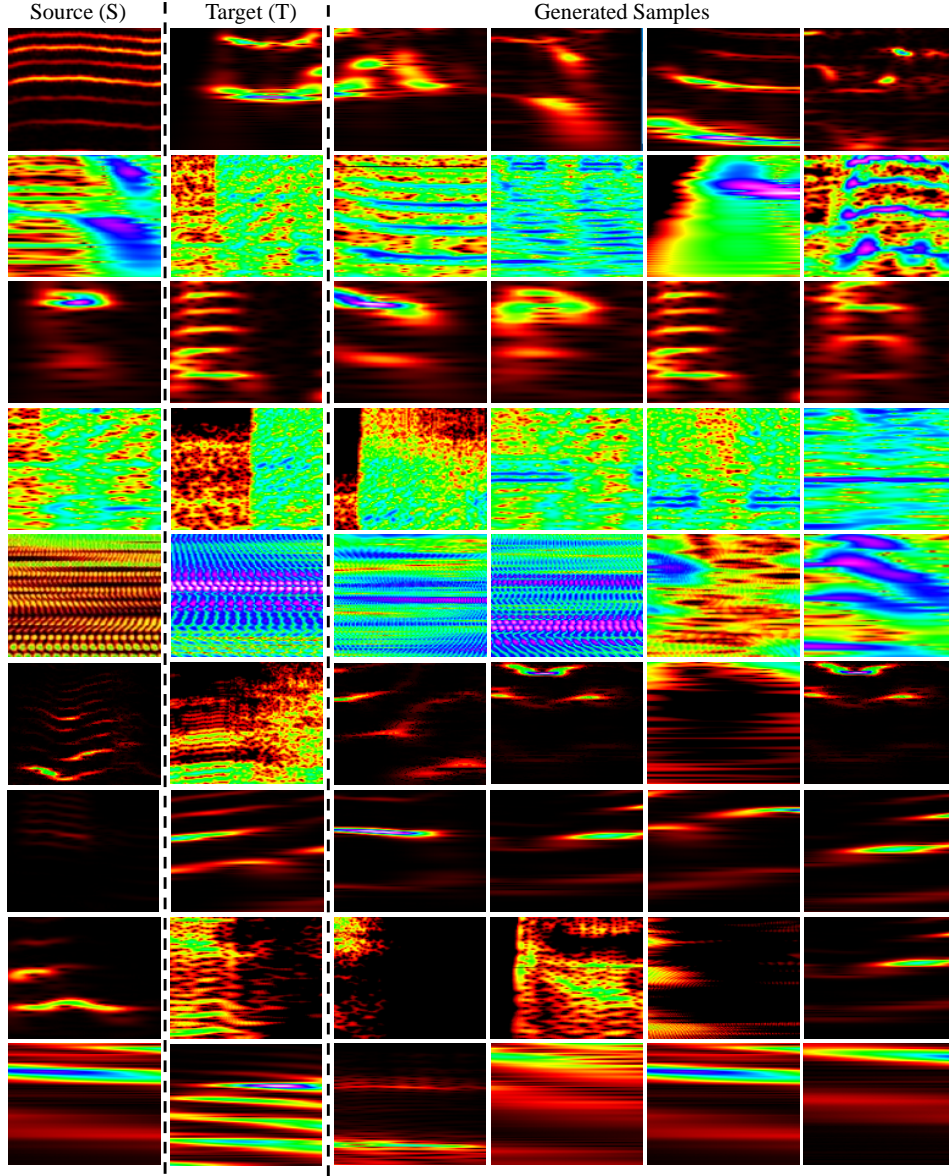


Figure 4: Generated spectrograms using cycle-consistent GAN for randomly drawn sources (S) and targets (T). The S s and T s shown in the top four rows indicate intra class image-to-image translation. Specifically, UrbanSound8K ($S = T$: sea waves), ESC-10 ($S = T$: person sneeze), ESC-50 ($S = T$: pouring water), and DCASE-2017 ($S = T$: office). Sources and targets for inter class translation are shown in the five bottom rows as in UrbanSound8K (S : sea waves, T : rain), ESC-10 (S : person sneeze, T : helicopter), ESC-50 (S : wind, T : pouring water), and DCASE-2017 (S : cafe, T : office).

	AI	CA	CH	DO	DR	EN	GU	JA	SI	SM
AI	0.68	0.00	0.02	0.01	0.05	0.14	0.01	0.04	0.02	0.03
CA	0.00	0.77	0.02	0.02	0.00	0.00	0.00	0.05	0.07	0.07
CH	0.07	0.05	0.31	0.09	0.04	0.03	0.02	0.04	0.15	0.20
DO	0.06	0.04	0.03	0.68	0.04	0.02	0.03	0.00	0.05	0.05
DR	0.02	0.04	0.02	0.02	0.74	0.01	0.01	0.10	0.04	0.00
EN	0.04	0.00	0.03	0.02	0.01	0.78	0.02	0.06	0.01	0.03
GU	0.00	0.03	0.00	0.03	0.00	0.00	0.95	0.00	0.00	0.00
JA	0.01	0.01	0.00	0.00	0.05	0.03	0.00	0.90	0.00	0.00
SI	0.03	0.05	0.03	0.02	0.02	0.01	0.03	0.01	0.77	0.01
SM	0.03	0.08	0.06	0.09	0.08	0.08	0.01	0.04	0.06	0.47

(a)

	AI	CA	CH	DO	DR	EN	GU	JA	SI	SM
AI	0.89	0.01	0.00	0.02	0.01	0.04	0.00	0.01	0.02	0.00
CA	0.01	0.91	0.00	0.01	0.02	0.00	0.01	0.01	0.00	0.02
CH	0.00	0.01	0.91	0.03	0.00	0.01	0.00	0.00	0.1	0.03
DO	0.00	0.00	0.01	0.96	0.1	0.00	0.00	0.00	0.01	0.01
DR	0.00	0.01	0.00	0.02	0.95	0.01	0.00	0.02	0.00	0.00
EN	0.01	0.00	0.00	0.01	0.00	0.96	0.02	0.00	0.00	0.01
GU	0.01	0.00	0.00	0.00	0.01	0.00	0.97	0.01	0.00	0.00
JA	0.02	0.00	0.00	0.00	0.00	0.00	0.00	0.98	0.00	0.00
SI	0.00	0.01	0.03	0.00	0.01	0.00	0.00	0.00	0.95	0.00
SM	0.00	0.01	0.02	0.00	0.00	0.00	0.01	0.00	0.00	0.94

(b)

Figure 5: The confusion matrix of our proposed classification scenario: (a) without and (b) with Cycle-Consistent GAN augmentation on the UrbanSound8K dataset. The values shown in bold face indicate the best recognition accuracy in a 5-fold cross validation setup.

and between "SI" and "CH" (15% + 3%). Some visual examples of the generated spectrograms using Cycle-Consistent GAN is depicted in Fig. 4. This figure interestingly showcases the high capability of the Cycle-Consistent GAN for producing structurally similar spectrograms even when the source and target are not similar to each other in human eyes perspective.

After finishing both inter and intra data augmentation processes, we train again the random forests with varying values of tree sizes. The best number of trees for ESC-10, ESC-50, UrbanSound8K, and DCASE-2017 were obtained at 2,000, 1,864, 2,500, 2,496, respectively with minimum AUC metrics (one-vs-all). Fig. 5b shows the performance of the learned trees on the UrbanSound8K dataset augmented with the proposed Cycle-Consistent GAN approach. The results are highly improved compared to the trees trained on codebooks without data augmentation (Fig. 5a). This shows the importance of data augmentation for extracting more discriminating features.

Table 3 compares the performance of the proposed classification approach with the state-of-the-art pretrained classifiers (AlexNet and GoogLeNet) on environmental sound datasets following the transfer learning and fine tuning strategy explained in [70]. It is worth mentioning that, these two pretrained networks have been fine-tuned on the 2D aggregation (pooling) of STFT, MFCC, and CRP. As Table 3 shows, our approach outperforms advanced deep learning models for all environmental sound datasets. One clear outcome of Table 3 is that, not only the GAN theory could help us to build robust classifiers, but also can highlight another traditional classifier’s performance. Furthermore, for better comparison of the achieved values, box-plots of these classifiers are shown in Fig. 6. With respect to these box-plots for all the four benchmarking datasets, the proposed approach using our architectures for data augmentation achieved the highest maximum, mean, minimum, and median accuracy. These plots also confirm that the proposed approach with data augmentation outperforms AlexNet and GoogLeNet since it provides the highest statistical measures except for the ESC-50 dataset; and there are no outliers.

Table 3: Comparing our proposed approach with and without high-level augmentation (DA) with GoogLeNet and AlexNet in terms of mean accuracy. Comparison has been made in a 5-fold cross validation setup on three standard benchmarking environmental sound datasets. The best results are shown in bold faces. Note that, AlexNet and GoogLeNet are trained on the 2D aggregation (pooling) of STFT, MFCC, and CRP.

Dataset	Mean Accuracy			
	GoogLeNet	AlexNet	Proposed Approach	
			Without DA	With DA
ESC-10	0.83	0.83	0.72	0.87
ESC-50	0.71	0.64	0.55	0.77
UrbanSound8K	0.91	0.90	0.73	0.94
DCASE-2017	0.64	0.62	0.66	0.75

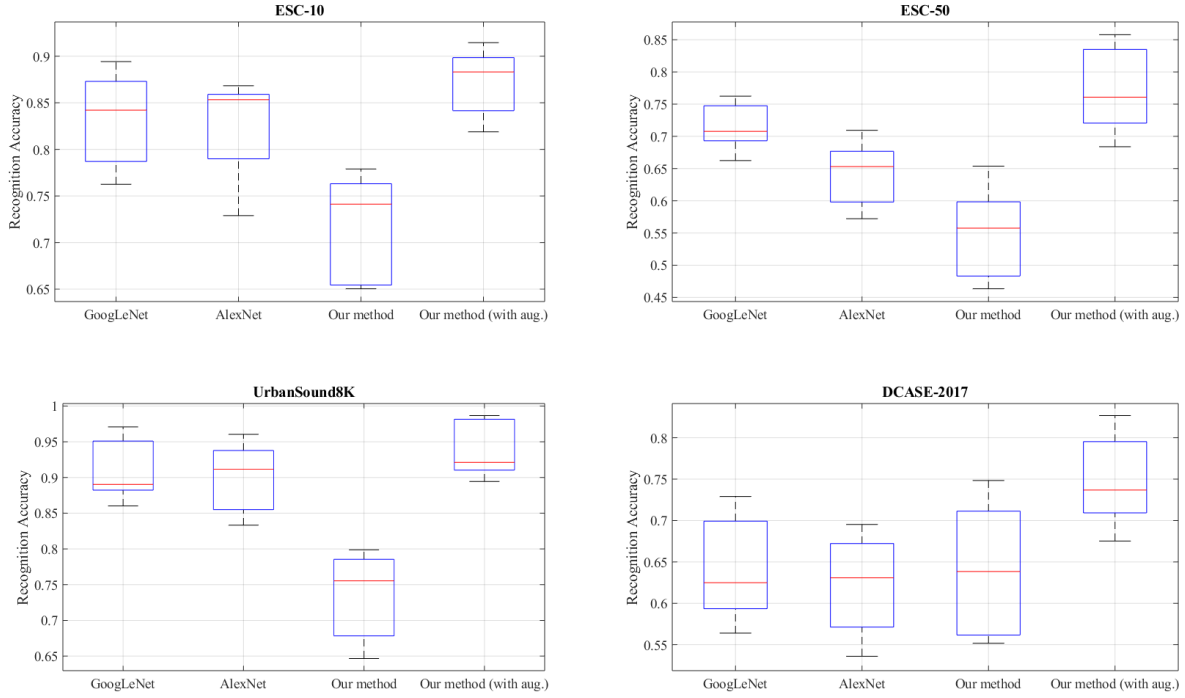


Figure 6: Box-plots of the approaches from Table 3 in a 5-fold cross validation setup for ESC-10, ESC-50, UrbanSound8K and DCASE-2017 datasets.

In order to investigate the statistical significance of the achieved recognition performances reported in Table 3, we run Friedman’s test which is the non-parametric version of the one-way ANOVA with some limited repeated measures [71]. Upon 19 runs (degrees of freedom), we could reach the p -value of 0.05 on average, which shows the high performance of the proposed approach.

The last experiment in this research work is measuring performances of the GoogLeNet and AlexNet on the augmented DWT spectrograms using our proposed cycle-consistent GAN architecture. We fine-tuned these two dense pretrained networks in four augmented datasets of ESC-10, ESC-50, UrbanSound8K, and DCASE-2017. Table 4 shows the achieved results. The results show the importance of high-level data augmentation for environmental sound classification purposes. With respect to the values reported in this table, GoogLeNet trained on the augmented DWT spectrogram outperforms our proposed classification method on ESC-50 dataset. Moreover, the performance of these two ConvNets are very close to our classification scheme.

Table 4: Recognition accuracy of two ConvNets on the augmented DWT spectrograms of four benchmarking datasets. The 5-fold cross validation setup is applied. The bold value indicates the best recognition performance. The reported mean confidence refers to the probabilities of the softmax layer.

Dataset	Mean Accuracy (%)		Mean Confidence (%)
	GoogLeNet	AlexNet	
ESC-10	0.86	0.85	80.32
ESC-50	0.78	0.75	81.11
UrbanSound8K	0.93	0.93	90.29
DCASE-2017	0.73	0.74	83.76

Table 5 summarizes the comparison between all approaches with and without the proposed data augmentation through an average ranking [72] according to the measured mean accuracy. The proposed approach with data augmentation has the best rank among all considered approaches, followed by the GoogLeNet with data augmentation, AlexNet with data augmentation, GoogLeNet, AlexNet, and the proposed approach without data augmentation. The most impressive improvement due to the proposed data augmentation is observed for the proposed approach which moves from the last (6th) to

the top spot (1st).

Approach	\bar{r}	Rank
Proposed Approach (DA)	1.25	1
Proposed Approach	5.00	6
GoogLeNet (DA)	1.50	2
GoogLeNet	4.50	4
AlexNet (DA)	2.50	3
AlexNet	4.75	5

Table 5: Average ranking (\bar{r}) considering the best mean accuracy for the four datasets [72].

Table 6 shows the mean classification accuracy of the proposed approach with and without data augmentation as well as the results obtained by other state-of-the-art approaches described in the literature. The proposed approach achieved the highest mean accuracy for all datasets, but ESC-10. However, the Soundnet [8] learns a multimodal representation from a very-large dataset of unlabeled videos which are further used with an SVM. Therefore, the proposed approach outperforms most of the approaches trained on handcrafted features or trained on both 1D signal and 2D spectrograms.

Table 6: Mean accuracy of different environmental sound classification approaches in UrbanSound8K, ESC-10, ESC-50 and DCASE-2017 datasets with and without data augmentation (DA). Values are rounded in two floating point precision.

Approach	Mean Accuracy			
	UrbanSound8K	ESC-10	ESC-50	DCASE-2017
Proposed Approach (DA)	0.94	0.87	0.77	0.75
SoundNet [8]	0.79	0.92	0.74	NA
SB-ConvNets (DA) [12]	0.79	0.77	0.54	0.45
MoE [73]	0.77	NA	NA	NA
SKM (DA) [4]	0.76	0.74	0.56	0.43
SKM [4]	0.74	0.71	0.52	0.36
Proposed Approach	0.73	0.71	0.55	0.66
PiczakConvNets [11]	0.73	0.80	0.65	0.52
SB-ConvNets [12]	0.73	0.72	0.49	0.41
MultiTemp [74]	0.72	0.74	0.71	0.73
VGG [75]	0.70	NA	NA	NA

NA: Not Available.

6. Conclusion

In this paper we showed how to structurally augment imbalanced environmental sound datasets in a high-level fashion using cycle-consistent generative adversarial network. Our proposed augmentation framework applies identity mapping to discriminator networks, which alongside using the least-squared optimization criterion solves the gradient vanishing problem and produces nice looking spectrograms. We form a codebook with visual words extracted by SURF detectors from augmented spectrograms organized in a unit distance to each other in a setup imposed by the K -Means++ algorithm. A finely trained random forest classifier with 2,000 trees on average, on the obtained codebooks could outperform the cutting-edge AlexNet and GoogLeNet for benchmarking datasets of ESC-10, ESC-50, UrbanSound8K, and DCASE-2017. Furthermore, as the experimental results indicate, besides outperforming advanced deep models as GoogLeNet and AlexNet, our unsupervised feature learning using our proposed architecture for cycle-consistent GAN compares favorably with most of the current approaches to environmental sound classification.

The proposed high-level data augmentation is also able to produce consistent samples that keep structural significance which is much more meaningful compared to other approaches such as simple image transformations or even conventional GANs. Both former data augmentation approaches do not allow control of the generated samples, especially regarding their structural consistency. The experimental results have shown that the proposed approach for data augmentation can even improve the performance of the pretrained ConvNets for the environmental sound classification task.

The proposed architecture for data augmentation can be extended to other datasets using finely-tuned and updated architectures for generators and discriminators. We would like to extend this work for structured datasets such as music datasets and evaluate the performance of our proposed classification scenario.

With respect to the experiments that have been carried out, the cycle-consistent GAN outperforms the regular GAN since for the latter, we do not have much control

over consistency of the source and target inputs. Overall, high-level data augmentation using GANs translates structural components from sample to sample where low-level augmentation algorithms cannot.

Our classification approach is a promising step towards building reliable classifiers for more complex environmental sound datasets containing many different waveforms in terms of sound production mechanism. For the future work, we are interested in implementing Wasserstein GAN [52] for image-to-image translation since, it not only is more optimized in optimization-wise way, but also suffers less from oversmoothing effects on the spectrograms generated. This might improve further the performance of the classifier.

Unsupervised feature learning has shown great competence in classifying 2D representations of the environmental sound datasets and even outperformed advanced deep learning models such as AlexNet and GoogLeNet. In addition to improving Spherical K -means++ algorithm for environmental sound classification, we would like to measure the performance of other unsupervised algorithms on the augmented DWT datasets so as to understand the strength of these classifiers.

References

- [1] Selina Chu, Shrikanth Narayanan, and C-C Jay Kuo. Environmental sound recognition with time–frequency audio features. IEEE Transactions on Audio, Speech, and Language Processing, 17(6):1142–1158, 2009.
- [2] Regunathan Radhakrishnan, Ajay Divakaran, and A Smaragdis. Audio analysis for surveillance applications. In Applications of Signal Processing to Audio and Acoustics, 2005. IEEE Workshop on, pages 158–161. IEEE, 2005.
- [3] Min Xu, Changsheng Xu, Lingyu Duan, Jesse S Jin, and Suhuai Luo. Audio keywords generation for sports video analysis. ACM Transactions on Multimedia Computing, Communications, and Applications (TOMM), 4(2):11, 2008.
- [4] Justin Salamon and Juan Pablo Bello. Unsupervised feature learning for urban sound classification. In Acoustics, Speech and Signal Processing (ICASSP), 2015 IEEE International Conference on, pages 171–175. IEEE, 2015.
- [5] S Noda, S Mori, F Ishibashi, and K Itomi. Effect of coils on natural frequencies of stator cores in small induction motors. IEEE transactions on energy conversion, (1):93–99, 1987.

- [6] Sourish Chaudhuri and Bhiksha Raj. Unsupervised hierarchical structure induction for deeper semantic analysis of audio. In Acoustics, Speech and Signal Processing (ICASSP), 2013 IEEE International Conference on, pages 833–837. IEEE, 2013.
- [7] Daniel PW Ellis and Keansub Lee. Minimal-impact audio-based personal archives. In Proceedings of the the 1st ACM workshop on Continuous archival and retrieval of personal experiences, pages 39–47. ACM, 2004.
- [8] Yusuf Aytar, Carl Vondrick, and Antonio Torralba. Soundnet: Learning sound representations from unlabeled video. In Advances in Neural Information Processing Systems, pages 892–900, 2016.
- [9] Wei Dai, Chia Dai, Shuhui Qu, Juncheng Li, and Samarjit Das. Very deep convolutional neural networks for raw waveforms. In Acoustics, Speech and Signal Processing (ICASSP), 2017 IEEE International Conference on, pages 421–425. IEEE, 2017.
- [10] Seongkyu Mun, Sangwook Park, David K Han, and Hanseok Ko. Generative adversarial network based acoustic scene training set augmentation and selection using svm hyper-plane. Proc. DCASE, pages 93–97, 2017.
- [11] Karol J Piczak. Environmental sound classification with convolutional neural networks. In Machine Learning for Signal Processing (MLSP), 2015 IEEE 25th International Workshop on, pages 1–6. IEEE, 2015.
- [12] Justin Salamon and Juan Pablo Bello. Deep convolutional neural networks and data augmentation for environmental sound classification. IEEE Signal Processing Letters, 24(3):279–283, 2017.
- [13] Yuji Tokozume and Tatsuya Harada. Learning environmental sounds with end-to-end convolutional neural network. In Acoustics, Speech and Signal Processing (ICASSP), 2017 IEEE International Conference on, pages 2721–2725. IEEE, 2017.
- [14] Lie Lu, Hong-Jiang Zhang, and Hao Jiang. Content analysis for audio classification and segmentation. IEEE Transactions on speech and audio processing, 10(7):504–516, 2002.
- [15] George Tzanetakis and Perry Cook. Musical genre classification of audio signals. IEEE Transactions on speech and audio processing, 10(5):293–302, 2002.
- [16] Daniel PW Ellis. Classifying music audio with timbral and chroma features. In Ismir, volume 7, pages 339–340, 2007.
- [17] Beth Logan et al. Mel frequency cepstral coefficients for music modeling. In ISMIR, volume 270, pages 1–11, 2000.
- [18] Julius O Smith et al. Spectral audio signal processing, volume 1334027739. W3K, 2011.
- [19] Joan Serra, Xavier Serra, and Ralph G Andrzejak. Cross recurrence quantification for cover song identification. New Journal of Physics, 11(9):093017, 2009.

- [20] Patrick J Van Fleet. Discrete wavelet transformations: An elementary approach with applications. John Wiley & Sons, 2011.
- [21] Michalis Papakostas, Evangelos Spyrou, Theodoros Giannakopoulos, Giorgos Siantikos, Dimitrios Sgouropoulos, Phivos Mylonas, and Fillia Makedon. Deep visual attributes vs. hand-crafted audio features on multidomain speech emotion recognition. Computation, 5(2):26, 2017.
- [22] Ömer Nezih Gerek and Dogan Gökhan Ece. Compression of power quality event data using 2d representation. Electric Power Systems Research, 78(6):1047–1052, 2008.
- [23] Rui Cai, Lie Lu, Alan Hanjalic, Hong-Jiang Zhang, and Lian-Hong Cai. A flexible framework for key audio effects detection and auditory context inference. IEEE Transactions on audio, speech, and language processing, 14(3):1026–1039, 2006.
- [24] Todor Ganchev, Nikos Fakotakis, and George Kokkinakis. Comparative evaluation of various mfcc implementations on the speaker verification task. In Proceedings of the SPECOM, volume 1, pages 191–194, 2005.
- [25] Toni Heittola, Annamaria Mesaros, Antti Eronen, and Tuomas Virtanen. Context-dependent sound event detection. EURASIP Journal on Audio, Speech, and Music Processing, 2013(1):1, 2013.
- [26] Juan Ignacio Godino-Llorente, Pedro Gomez-Vilda, and Manuel Blanco-Velasco. Dimensionality reduction of a pathological voice quality assessment system based on gaussian mixture models and short-term cepstral parameters. IEEE transactions on biomedical engineering, 53(10):1943–1953, 2006.
- [27] MJF Gales and S Young. An improved approach to the hidden markov model decomposition of speech and noise. In Acoustics, speech, and signal processing, 1992. ICASSP-92., 1992 IEEE international conference on, volume 1, pages 233–236. IEEE, 1992.
- [28] Antti J Eronen, Vesa T Peltonen, Juha T Tuomi, Anssi P Klapuri, Seppo Fagerlund, Timo Sorsa, Gaëtan Lorho, and Jyri Huopaniemi. Audio-based context recognition. IEEE Transactions on Audio, Speech, and Language Processing, 14(1):321–329, 2006.
- [29] Li Deng, Geoffrey Hinton, and Brian Kingsbury. New types of deep neural network learning for speech recognition and related applications: An overview. In Acoustics, Speech and Signal Processing (ICASSP), 2013 IEEE International Conference on, pages 8599–8603. IEEE, 2013.
- [30] Courtenay V Cotton and Daniel PW Ellis. Spectral vs. spectro-temporal features for acoustic event detection. In Applications of Signal Processing to Audio and Acoustics (WASPAA), 2011 IEEE Workshop on, pages 69–72. IEEE, 2011.
- [31] Karol J Piczak. Esc: Dataset for environmental sound classification. In Proceedings of the 23rd ACM international conference on Multimedia, pages 1015–1018. ACM, 2015.

- [32] Dimitri Palaz, Mathew Magimai Doss, and Ronan Collobert. Convolutional neural networks-based continuous speech recognition using raw speech signal. In Acoustics, Speech and Signal Processing (ICASSP), 2015 IEEE International Conference on, pages 4295–4299. IEEE, 2015.
- [33] Zheng Weiping, Yi Jiantao, Xing Xiaotao, Liu Xiangtao, and Peng Shaohu. Acoustic scene classification using deep convolutional neural network and multiple spectrograms fusion. In Detection and Classification of Acoustic Scenes and Events 2017 Workshop (DCASE2017), 2017.
- [34] Venkatesh Boddapati, Andrej Petef, Jim Rasmusson, and Lars Lundberg. Classifying environmental sounds using image recognition networks. Procedia Computer Science, 112: 2048–2056, 2017.
- [35] Lonce Wyse. Audio spectrogram representations for processing with convolutional neural networks. arXiv preprint arXiv:1706.09559, 2017.
- [36] Justin Salamon and Juan Pablo Bello. Feature learning with deep scattering for urban sound analysis. In Signal Processing Conference (EUSIPCO), 2015 23rd European, pages 724–728. IEEE, 2015.
- [37] Dan C Cireşan, Ueli Meier, Jonathan Masci, Luca M Gambardella, and Jürgen Schmidhuber. High-performance neural networks for visual object classification. arXiv preprint arXiv:1102.0183, 2011.
- [38] Xinyue Zhu, Yifan Liu, Jiahong Li, Tao Wan, and Zengchang Qin. Emotion classification with data augmentation using generative adversarial networks. In Pacific-Asia Conference on Knowledge Discovery and Data Mining, pages 349–360. Springer, 2018.
- [39] Patrice Y Simard, Dave Steinkraus, and John C Platt. Best practices for convolutional neural networks applied to visual document analysis. In null, page 958. IEEE, 2003.
- [40] Alex Krizhevsky, Ilya Sutskever, and Geoffrey E Hinton. Imagenet classification with deep convolutional neural networks. In Advances in neural information processing systems, pages 1097–1105, 2012.
- [41] Søren Hauberg, Oren Freifeld, Anders Boesen Lindbo Larsen, John Fisher, and Lars Hansen. Dreaming more data: Class-dependent distributions over diffeomorphisms for learned data augmentation. In Artificial Intelligence and Statistics, pages 342–350, 2016.
- [42] Mandar Dixit, Roland Kwitt, Marc Niethammer, and Nuno Vasconcelos. Aga: Attribute-guided augmentation. In Proceedings of the IEEE Conference on Computer Vision and Pattern Recognition, pages 7455–7463, 2017.
- [43] Zhou Wang, Alan C Bovik, Hamid R Sheikh, and Eero P Simoncelli. Image quality assessment: from error visibility to structural similarity. IEEE transactions on image processing, 13(4):600–612, 2004.

- [44] Brian McFee, Eric J Humphrey, and Juan Pablo Bello. A software framework for musical data augmentation. In ISMIR, pages 248–254, 2015.
- [45] Steve Hanov. Wavelet sound explorer software. <http://stevehanov.ca/wavelet/>, 2008.
- [46] José C Segura, M Carmen Benítez, Ángel de la Torre, and Antonio J Rubio. Feature extraction combining spectral noise reduction and cepstral histogram equalization for robust asr. In Seventh International Conference on Spoken Language Processing, 2002.
- [47] Rafael C Gonzalez and Richard E Woods. Digital image processing second edition. Beijing: Publishing House of Electronics Industry, 455, 2002.
- [48] Phillip Isola, Jun-Yan Zhu, Tinghui Zhou, and Alexei A Efros. Image-to-image translation with conditional adversarial networks. arXiv preprint, 2017.
- [49] Jun-Yan Zhu, Taesung Park, Phillip Isola, and Alexei A Efros. Unpaired image-to-image translation using cycle-consistent adversarial networks. arXiv preprint, 2017.
- [50] J. Deng, W. Dong, R. Socher, L.-J. Li, K. Li, and L. Fei-Fei. ImageNet: A Large-Scale Hierarchical Image Database. In CVPR09, 2009.
- [51] Xinyue Zhu, Yifan Liu, Zengchang Qin, and Jiahong Li. Data augmentation in emotion classification using generative adversarial networks. arXiv preprint arXiv:1711.00648, 2017.
- [52] Martin Arjovsky, Soumith Chintala, and Léon Bottou. Wasserstein gan. arXiv preprint arXiv:1701.07875, 2017.
- [53] Xudong Mao, Qing Li, Haoran Xie, Raymond YK Lau, Zhen Wang, and Stephen Paul Smolley. Least squares generative adversarial networks. In Computer Vision (ICCV), 2017 IEEE International Conference on, pages 2813–2821. IEEE, 2017.
- [54] Ian Goodfellow, Jean Pouget-Abadie, Mehdi Mirza, Bing Xu, David Warde-Farley, Sherjil Ozair, Aaron Courville, and Yoshua Bengio. Generative adversarial nets. In Advances in neural information processing systems, pages 2672–2680, 2014.
- [55] Quan Hoang, Tu Dinh Nguyen, Trung Le, and Dinh Phung. Mgan: Training generative adversarial nets with multiple generators. 2018.
- [56] Kaiming He, Xiangyu Zhang, Shaoqing Ren, and Jian Sun. Deep residual learning for image recognition. In Proceedings of the IEEE conference on computer vision and pattern recognition, pages 770–778, 2016.
- [57] Herbert Bay, Tinne Tuytelaars, and Luc Van Gool. Surf: Speeded up robust features. In European conference on computer vision, pages 404–417. Springer, 2006.
- [58] David G Lowe. Object recognition from local scale-invariant features. In Computer vision, 1999. The proceedings of the seventh IEEE international conference on, volume 2, pages 1150–1157. Ieee, 1999.

- [59] Yonatan Vaizman, Brian McFee, and Gert Lanckriet. Codebook-based audio feature representation for music information retrieval. IEEE/ACM Transactions on Audio, Speech and Language Processing (TASLP), 22(10):1483–1493, 2014.
- [60] David Arthur and Sergei Vassilvitskii. k-means++: The advantages of careful seeding. In Proceedings of the eighteenth annual ACM-SIAM symposium on Discrete algorithms, pages 1027–1035. Society for Industrial and Applied Mathematics, 2007.
- [61] Inderjit S Dhillon and Dharmendra S Modha. Concept decompositions for large sparse text data using clustering. Machine learning, 42(1-2):143–175, 2001.
- [62] Adam Coates and Andrew Y Ng. Learning feature representations with k-means. In Neural networks: Tricks of the trade, pages 561–580. Springer, 2012.
- [63] Yasunori Endo and Sadaaki Miyamoto. Spherical k-means++ clustering. In Modeling Decisions for Artificial Intelligence, pages 103–114. Springer, 2015.
- [64] Dan Stowell and Mark D Plumbly. Automatic large-scale classification of bird sounds is strongly improved by unsupervised feature learning. PeerJ, 2:e488, 2014.
- [65] Sander Dieleman and Benjamin Schrauwen. Multiscale approaches to music audio feature learning. In 14th International Society for Music Information Retrieval Conference (ISMIR-2013), pages 116–121. Pontifícia Universidade Católica do Paraná, 2013.
- [66] Leo Breiman. Random forests. Machine learning, 45(1):5–32, 2001.
- [67] Justin Salamon, Christopher Jacoby, and Juan Pablo Bello. A dataset and taxonomy for urban sound research. In Proceedings of the 22nd ACM international conference on Multimedia, pages 1041–1044. ACM, 2014.
- [68] D Ulyanov, A Vedaldi, and VS Lempitsky. Instance normalization: the missing ingredient for fast stylization. corr abs/1607.08022 (2016).
- [69] Ishaan Gulrajani, Faruk Ahmed, Martin Arjovsky, Vincent Dumoulin, and Aaron C Courville. Improved training of wasserstein gans. In Advances in Neural Information Processing Systems, pages 5767–5777, 2017.
- [70] Anurag Kumar, Maksim Khadkevich, and Christian Fügen. Knowledge transfer from weakly labeled audio using convolutional neural network for sound events and scenes. In 2018 IEEE International Conference on Acoustics, Speech and Signal Processing (ICASSP), pages 326–330. IEEE, 2018.
- [71] Robert V Hogg and Johannes Ledolter. Engineering statistics. Macmillan Pub Co, 1987.
- [72] Pavel B. Brazdil and Carlos Soares. A Comparison of Ranking Methods for Classification Algorithm Selection. In Machine Learning: ECML 2000, volume 1810, pages 63–75. 2000.
- [73] Jiaying Ye, Takumi Kobayashi, and Masahiro Murakawa. Urban sound event classification based on local and global features aggregation. Applied Acoustics, 117:246–256, 2017.

- [74] Boqing Zhu, Kele Xu, Dezhi Wang, Lilun Zhang, Bo Li, and Yuxing Peng. Environmental Sound Classification Based on Multi-temporal Resolution Convolutional Neural Network Combining with Multi-level Features. volume 9314, pages 528–537. 2018. ISBN 978-3-319-24074-9. doi: 10.1007/978-3-030-00767-6_49. URL http://link.springer.com/10.1007/978-3-319-24075-6http://link.springer.com/10.1007/978-3-030-00767-6_{_}49.
- [75] Jordi Pons and Xavier Serra. Randomly weighted CNNs for (music) audio classification. 2018. URL <http://arxiv.org/abs/1805.00237>.